

Eight New Ultramassive Black Hole Masses confirm Best Correlation with Galaxy Core Sizes

STEFANO DE NICOLA,^{1,2} JENS THOMAS,^{2,1} ROBERTO P. SAGLIA,^{2,1} MATTHIAS KLUGE,² JAN SNIGULA,² AND
RALF BENDER^{1,2}

¹ *Universitäts-Sternwarte Muenchen, Scheinerstrasse 1, D-81679, Munich, Germany*

² *Max-Planck Institute for Extraterrestrial Physics, Giessenbachstrasse 1, D-85748, Garching (Germany)*

ABSTRACT

We analyse black-hole scaling relations at the high-mass end, focusing in particular on the regime of ultra-massive black holes, $M_{\text{BH}} > 10^{10} M_{\odot}$ (UMBHs). In a sample of 16 Brightest Cluster Galaxies (BCGs) without previous black-hole mass measurements we discover 8 UMBHs based on direct dynamical detections with triaxial Schwarzschild models. This first sample of triaxial black-hole mass determinations increases the number of known UMBHs by a factor of two and dramatically increases the constraints for BH mass scaling relations at the high-mass end. We find that BCGs are outliers in the canonical BH- σ relation, while the size of their depleted cores — the central light-deficient region — is a much better unbiased predictor of the black hole mass and should be used as a proxy at the high-mass end. BCGs smoothly join the trend already established for massive core galaxies in previous studies. This also holds for tight correlations between core size and sphere-of-influence radius and core size and core density. All these relations strongly support the black-hole binary model for the formation of the centers of the most massive galaxies.

Keywords: Galaxies (573) — Cosmology (343)

1. INTRODUCTION

A currently accepted paradigm is that essentially every galaxy hosts a Supermassive Black Hole (SMBH). Given that SMBHs lie at galaxy centres — thus feeding from the same material as their hosts — there is a close connection between the growth of SMBHs and their host galaxies (J. Kormendy & L. C. Ho 2013). Indeed, several galaxy properties have been found to participate in tight scaling relations with the black hole mass M_{BH} . These include the galaxy velocity dispersion σ (L. Ferrarese & D. Merritt 2000; K. Gebhardt et al. 2000; S. Tremaine et al. 2002) and the mass (or luminosity) of the spheroidal component, M_{bulge} (L_{bulge} , J. Magorrian et al. 1998; A. Marconi & L. K. Hunt 2003). On the one hand, these scaling relations encode important information about the physical processes that link SMBH and galaxy evolution together over a large range of galaxy and SMBH masses. On the other hand, since direct dynamical SMBH mass determinations are still rare, these scaling relations are important practical tools to approximate black hole masses in large surveys or in galaxies with unresolved centres. Hence, more than one work has

raised the question which relation predicts M_{BH} most precisely, with agreement that σ is the most promising variable (J. Kormendy & L. C. Ho 2013; R. P. Saglia et al. 2016; R. C. E. van den Bosch 2016; F. Shankar et al. 2016; S. de Nicola et al. 2019; F. Shankar et al. 2025).

At the high-mass end galaxy mergers are no longer dissipational but predominantly gas-free without star formation and without dissipationally-driven feedback processes. Such mergers in general do not significantly increase σ (M. Boylan-Kolchin et al. 2006; T. Naab et al. 2009; J. Kormendy & R. Bender 2013; A. King & K. Pounds 2015). The most striking observational evidence for gas-poor merging is the fact that massive elliptical galaxies exhibit a light deficit at their center where the surface brightness (SB) profile flattens compared to an inward extrapolation of the J. L. Sérsic (1963) profile characteristic at large radii. Such galaxies are referred to as a "core-elliptical" (S. M. Faber et al. 1997; T. R. Lauer et al. 2007; S. P. Rusli et al. 2013; B. T. Dullo & A. W. Graham 2014; K. Mehrgan et al. 2019). The origin of these cores is explained by in-falling SMBHs of the progenitors that eject stars via gravitational slingshots (T. Ebisuzaki et al. 1991; D. Merritt 2006; J. Thomas

et al. 2014; A. Rantala et al. 2018, 2019; M. Frigo et al. 2021).

Because the formation history of these most massive galaxies is different, the nature of the black-hole scaling relations changes as well. The cores give rise to new, core-specific scaling relations governed by the dynamics of black-hole binaries. These relations are local, basically confined to the sphere-of-influence of the central black-hole binary or, later, the merged black hole. Indeed, the amount of light in the core (J. Kormendy & R. Bender 2009), the core size (T. R. Lauer et al. 2007) and sphere-of-influence size (J. Thomas et al. 2016), and the SB of the core itself (K. Mehrgan et al. 2019) have been discovered to scale tightly with the SMBH mass. Instead, the global scaling relations between M_{BH} and σ are expected to break down because the galaxy velocity dispersions saturate (T. Naab et al. 2009; J. Kormendy & R. Bender 2013).

Just like the classical scaling relations do allow to estimate M_{BH} for intermediate mass early-type galaxies, the local core correlations allow to estimate M_{BH} for massive galaxies, even with less scatter. Core sizes, for example, have led to the discovery of the most massive SMBH found so far (K. Mehrgan et al. 2019) in a galaxy where the classical scaling relations predict a SMBH ten times smaller than observed.

While the physical process behind these core correlations – dynamics of SMBH binaries in gas-poor mergers – is expected to be generic at the high-mass end, little is known about SMBHs with masses above $10^{10} M_{\odot}$, often called ultra-massive black holes (UMBHs). So far, only 7 UMBHs have been discovered (N. J. McConnell et al. 2012; J. Thomas et al. 2016; K. Mehrgan et al. 2019; B. Neureiter et al. 2023; J. W. Nightingale et al. 2023; S. de Nicola et al. 2024; C. R. Melo-Carneiro et al. 2025). Here, we analyse SMBH scaling relations for a sample of 16 BCGs that are candidate hosts of UMBHs together with massive core galaxies from the literature (S. P. Rusli et al. 2013; J. Thomas et al. 2016; K. Mehrgan et al. 2019). This is the first sample of UMBHs and the first sample of triaxial black-hole mass measurements. Throughout this paper, we identify the BCG by the cluster name.

2. SAMPLE AND DATA

Our base sample consists of 17 BCGs from the large collection of 170 local BCGs of (M. Kluge et al. 2020, 2021) with very deep g' -band Wendelstein (U. Hopp et al. 2010; F. Lang-Bardl et al. 2016) data. The galaxies were selected to be candidate hosts of UMBHs due to their large central cores larger than 1 kpc or their high mass, both known to correlate with M_{BH} (J.

Thomas et al. 2016; R. Saglia et al. 2024). One of them (A262) has already been published in a pilot study (S. de Nicola et al. 2024). Some of these galaxies have archival high-resolution HST data, for the others we obtained AO-aided photometry from the Large Binocular Telescope Observatory (LBTO). In addition, long-slit spectra along 4 different position angles were collected using the MODS instrument at LBTO. We perform triaxial orbit-based dynamical models to measure the masses of the black holes, stars and dark-matter halos (S. de Nicola et al. 2020; B. Neureiter et al. 2021; M. Lipka & J. Thomas 2021; J. Thomas & M. Lipka 2022). We complement this sample of galaxies with new black-hole measurements in the UMBHs regime with existing data of other massive core ellipticals from S. P. Rusli et al. (2013); J. Thomas et al. (2016); K. Mehrgan et al. (2019); R. Saglia et al. (2024).

For 13 BCGs we estimate the core size r_c using the break radius r_b through fitting PSF-convolved Core-Sérsic (I. Trujillo et al. 2004) profiles to the 1D SB profiles of the galaxies, extracted along the semimajor axes of the isophotes. The high-resolution data (HST or AO-assisted LBT, see de Nicola et al. in prep. for details) allow us to resolve the cores. For A292 and A1185 we measure r_c by computing the cusp radius r_γ , defined as $d\text{SB}/d\log r(r_\gamma) = -1/2$ (C. M. Carollo et al. 1997). Finally, for A2107 only a single Sersic fit is needed to fit the SB profile, meaning that the galaxy does not have a core.

We take M_{BH} from the triaxial dynamical models where we also determine the radius of the sphere of influence, r_{SOI} , defined as $M_{\text{BH}} = M_*(r \leq r_{\text{SOI}})$, where M_* is the stellar mass. We also calculate a velocity dispersion σ as

$$\sigma = \sum_i \nu_i(r_i) \times w_i(r_i) / \sum_i w_i(r_i), \quad (1)$$

summed over all radial bins, with $\nu = \sqrt{v^2 + \sigma^2}$ and v, σ the measured line-of-sight velocity and velocity dispersion. We take as weights $w_i(r) = 2\pi R I(r)$, where R is the radius of the i -th bin and $I(r)$ the surface intensity. A detailed description of the photometric and spectroscopic data, the Core-Sérsic fits, the kinematic extraction of non-parametric LOSVDs with our new fitting code WINGFIT (K. Mehrgan et al. 2023, Thomas in prep.) and a description of the dynamical models is provided in a companion paper (de Nicola et al. in prep.).

3. SCALING RELATIONS

Our novel 8 UMBH detections more than double the number of such systems, allowing for a statistically sig-

nificant investigation of the classical scaling relations between black holes and host galaxies such as the $M_{\text{BH}} - \sigma$ and those involving core ellipticals at the very high-mass end, providing insights in the coevolution of these systems and their hosts. We analyze the canonical $M_{\text{BH}} - \sigma$ correlation before focusing on r_c and its correlations with M_{BH} , the sphere-of-influence r_{SOI} , the stellar mass M_* and the core density ρ_{core} , along with a possible correlation between M_{BH} and the mass deficit inside the core M_{def} . We finally speculate about the existence of UMBHs in core-less galaxies.

All the data needed to generate the plots presented in the next sections are reported in Tab. 1. For all other galaxies we take the respective data from the literature (C. R. Melo-Carneiro et al. 2025; R. Saglia et al. 2024; S. de Nicola et al. 2024; B. Neureiter et al. 2023; K. Mehrgan et al. 2019; J. Thomas et al. 2016; S. P. Rusli et al. 2013).

3.1. The break-down of $M_{\text{BH}} - \sigma$

Core ellipticals do not follow the canonical $M_{\text{BH}} - \sigma$ scaling relation (see, e.g., R. P. Saglia et al. 2016; K. Mehrgan et al. 2019). BCGs, in particular, often show low velocity dispersions (M. Kluge & R. Bender 2023, de Nicola et al. in prep.): the $M_{\text{BH}} - \sigma$ relation would predict very small black holes with $M_{\text{BH}} < 10^9 M_\odot$ for these galaxies. In Fig. 1, we show the dispersions and black-hole masses of our galaxies together with the best-fit relation for less massive galaxies and additional objects from R. Saglia et al. (2024) and references therein. The figure confirms that nearly all BCGs from our sample host overmassive BHs relative to the predictions of the canonical $M_{\text{BH}} - \sigma$ relation, and the effect is particularly severe due to the low σ values of most BCGs. Low velocity dispersions in massive ETGs fit into the dry merger scenario as discussed in the introduction.

3.2. $M_{\text{BH}} - r_c$

An inevitable consequence of dry merging between galaxies with supermassive black holes is core scouring through a combination of dynamical friction and gravitational slingshots (M. Frigo et al. 2021). At the end of this process the remnant galaxy has a diffuse central core with a shallow, almost constant surface brightness profile. It can be characterised by a core or break radius that defines the transition from an outer Sersic-like surface-brightness distribution to the core. The core typically follows a shallow power-law distribution. Previous studies have shown that massive elliptical galaxies with depleted stellar cores exhibit an almost linear relationship between the masses M_{BH} of their black holes and the size of the core (J. Thomas

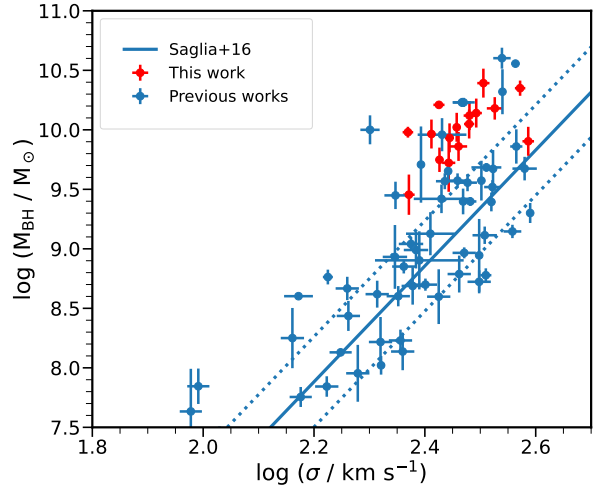


Figure 1. The $M_{\text{BH}} - \sigma$ relation with data from the literature (blue points) with our new measurements (red points). The solid line is the best-fit relation from R. P. Saglia et al. (2016) omitting pseudobulges, while the dotted lines enclose the intrinsic scatter $\varepsilon = 0.380 \pm 0.038$.

et al. 2016). Fig. 2 shows this relation for our new sample. It is clear that the relation extends to the regime of UMBHs. A comparison between Figs. 1 and 2 clearly demonstrates that σ is a bad predictor of M_{BH} at the high-mass end. Instead, the core size scales as tightly with M_{BH} at the high-mass end, as does the dispersion σ for intermediate-mass bulges.

We obtain a robust log-linear relation

$$\log \frac{M_{\text{BH}}}{M_\odot} = (0.916 \pm 0.081) \log \frac{r_c}{\text{kpc}} + (10.087 \pm 0.053) \quad (2)$$

with an intrinsic scatter of $\varepsilon = 0.222 \pm 0.035$. Nearly all data points fall within the intrinsic scatter of this relation, and the slope of this relation is similar to the slope observed in massive core galaxies (J. Thomas et al. 2016).

We observe two kinds of outliers in the $M_{\text{BH}} - r_b$ relation. The galaxy A240 is an example of an outlier with a too large core: simulations show that recoil kicks can generate very large cores compared to M_{BH} (A. Rawlings et al. 2025) if the recoil velocity is a factor of 2–3 higher than the escape velocity. While this is not the general case for our sample—our black holes correlate well with the core size—for galaxies such as A240, this mechanism could play a role. We discuss large BHs found in galaxies with small (or no) cores in Sec. 3.7.

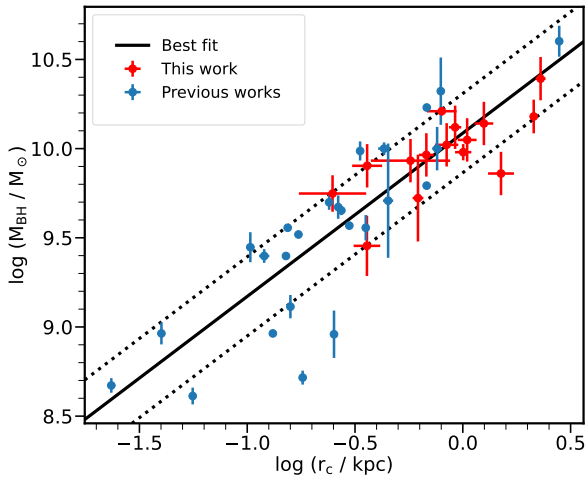


Figure 2. The M_{BH} -core size relation with data from the literature (blue points) with our new measurements (red circles). The solid and dotted lines are the best-fit line and the intrinsic scatter, respectively.

3.3. $M_{\text{BH}} - M_*$ and $r_c - M_*$

A classical scaling relation that is obeyed by core ellipticals is that between M_{BH} and the galaxy stellar mass M_* (R. Saglia et al. 2024). This tells us that the most massive BHs are found in the most massive galaxies, agreeing well with the picture of coevolution of BH and host galaxies (J. Kormendy & L. C. Ho 2013). We evaluate M_* in two ways:

- We take the total integrated magnitude M_V of M. Kluge et al. (2020) and turn this into a mass estimate using our dynamically estimated mass-to-light ratios (see de Nicola et al., in prep.);
- We evaluate the total luminosity by integrating the innermost Sersic component reported by M. Kluge et al. (2020) to fit the SB profile up to infinity.

The exact values are reported in Tab. 1. In the top panels of Fig. 3 we show the correlation of R. P. Saglia et al. (2016) with the points from R. Saglia et al. (2024) in blue and our BCGs plotted as red points. We see that contrarily to the $M_{\text{BH}} - \sigma$ relation, our core-ellipticals do follow this scaling relation. Instead, in the bottom panels of Fig. 3 we do the same for the $r_c - M_*$ correlation of R. Saglia et al. (2024). We see that the most BCGs agree well with this relation - this is expected given the tightness of the $M_{\text{BH}} - r_c$ relation - with few outliers for which M_* is too high. This might be due to contamination from ICL (M. Kluge et al. 2021). In fact,

the effect is mitigated by evaluating M_* using the innermost Sersic component rather than integrating the whole 2D profile (compare bottom panels). In particular, A399 has a very large M/L value, whereas A2319 has one of the smallest core radii of the sample. Moreover, M. Kluge et al. (2020) report a best-fit profile with only one Sersic component and very large effective radii: in this case, disentangling BCG and ICL becomes difficult.

We stress here the importance of these correlations: $r_c - M_*$ allows us to estimate the stellar mass of a galaxy only relying on photometric analysis, whereas $M_{\text{BH}} - M_*$ can be used to hunt UMBHs in core-less galaxies such as A2107 or A1201 (see also Sec. 3.7 below).

3.4. $r_{\text{SOI}} - r_c$

While the correlation between core size and black-hole mass discussed in the previous Sec. 3.2 seems natural - bigger black-holes carve out bigger cores - it is not a direct consequence of the black-hole binary model for core scouring. In fact, a purely dynamical argument supporting the formation of cores by SMBHs is provided by the very tight correlation between the size of the sphere of influence r_{SOI} , defined as $M_*(< r_{\text{SOI}}) = M_{\text{BH}}$, and the size of the core (J. Thomas et al. 2016). In Fig. 4 we demonstrate that this correlation also extends to the regime of UMBHs. The best-fit relation is

$$\log \frac{r_{\text{SOI}}}{\text{kpc}} = (0.960 \pm 0.060) \log \frac{r_c}{\text{kpc}} + (0.028 \pm 0.039) \quad (3)$$

with an intrinsic scatter of $\varepsilon = 0.161 \pm 0.026$. This is in very good agreement with the relation in J. Thomas et al. (2016). The fact that r_{SOI} and r_c are essentially identical provides the most direct link between the gravitational influence of the SMBHs and cores.

However, if we assume that the stellar density profile in the center is approximately a power-law

$$\rho = \rho_{\text{core}} \left(\frac{r}{r_c} \right)^{-\gamma}, \quad (4)$$

where $\rho_{\text{core}} = \frac{3M_*(r_c)}{4\pi r_c^3}$ is the mass density at the break radius r_c , then the enclosed stellar mass reads

$$M_*(r \leq r_c) = \frac{4\pi\rho_{\text{core}}}{3-\gamma} r_c^3. \quad (5)$$

If we now take into account the empirical fact that $r_{\text{SOI}} \approx r_c$ as discussed above (Eq. 3) and the definition of the sphere-of-influence then we directly obtain

$$M_{\text{BH}} \sim \frac{4\pi\rho_{\text{core}}}{3-\gamma} r_c^3. \quad (6)$$

This reflects that, physically, the core size can not be exclusively determined by M_{BH} . While the black-hole

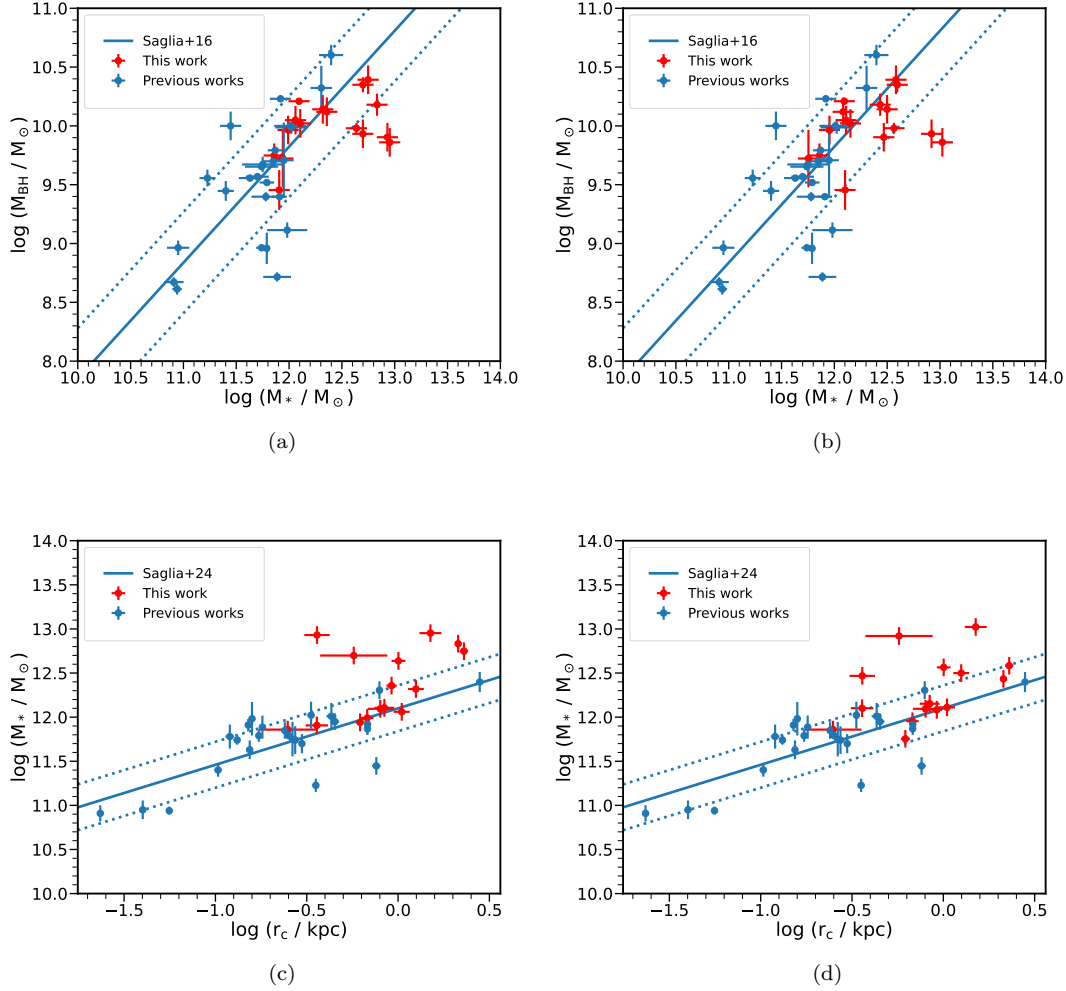


Figure 3. Same as Fig. 1 for the $M_{\text{BH}} - M_*$ and $M_* - r_b$ relations. In Figs. 3a and 3c the stellar mass has been estimated using the total V-band magnitude, whereas in Figs. 3b and 3d it comes from the integrated 1D best-fit Sersic profiles. In both cases the data are taken from Table 4 of M. Kluge et al. (2020); the best-fit relations and intrinsic scatters (blue lines) come from R. P. Saglia et al. (2016) (top panels) and R. Saglia et al. (2024) (bottom panels), respectively.

mass (in an equal mass merger) roughly defines the available gravitational energy of the binary, the size of the depleted core that can be produced as a result of the release of this energy will also depend on the binding energy of the progenitor centers, i.e. on the core density ρ_{core} .

3.5. $\rho_{\text{core}} - r_c$

In fact, Eq. 6 implies that any correlation between M_{BH} and r_c requires a *homology* in the progenitor galaxies, i.e. a correlation between ρ_{core} and r_c (variations in γ will only play a minor role, given that the range of γ in real galaxies is small compared to the range of ρ_{core} and r_c). In fact, if $\rho_{\text{core}} \sim r_c^\alpha$, then $M_{\text{BH}} \sim r_c^{(3+\alpha)}$. Thus, the almost linear relationship between M_{BH} and r_c observed in real galaxies (Eq. 2) leads to $\rho_{\text{core}} \sim r_c^{-2}$. In

Fig. 5 we show the core densities ρ_{core} and core sizes r_c of our sample galaxies explicitly. As expected, there is a strong correlation

$$\log \frac{\rho_{\text{core}}}{M_\odot \text{kpc}^{-3}} = (-2.08 \pm 0.11) \log \frac{r_c}{\text{kpc}} + (9.313 \pm 0.068). \quad (7)$$

with an intrinsic scatter of $\varepsilon = 0.272 \pm 0.043$. Eq. 7 is the 3d version of the observed tight scaling between the core surface brightness and core size (S. M. Faber et al. 1997). Fig. 5 suggests that the progenitors of the cores had a nearly universal central density profile with a slope of $\gamma \approx -2.1$. We do not know exactly when the final mergers take place which produce the depleted stellar cores, but we note that this estimated progenitor slope is consistent with the peak of the central slopes of power-law ellipticals in the local universe (T. R. Lauer

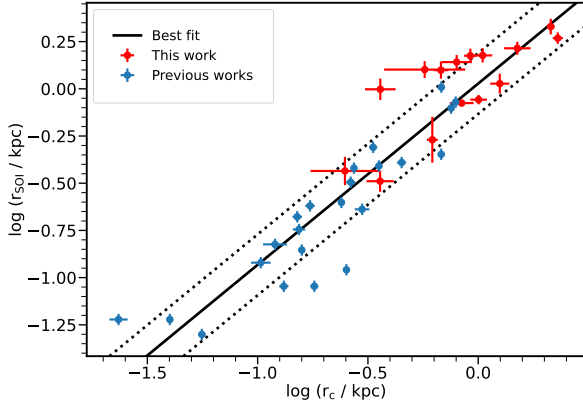


Figure 4. Same as Fig. 2 but the correlation between black hole sphere of influence r_{SOI} and core size r_c is shown.

et al. 2007). The simulations of elliptical galaxies with SMBHs of A. Rantala et al. (2018) also showed that the central density slopes of the progenitor galaxies determine the slope of the final correlation between black-hole mass and core size in the remnants. They also showed that progenitor slopes steeper than $\gamma < -1.5$ are required for the remnants to follow a correlation between black-hole mass and core size with a similar slope as the one observed in real galaxies. Density slopes near $\gamma \approx -2$ are also consistent with the properties of elliptical galaxies as a whole (M. Cappellari 2016) (see also references therein).

3.6. $M_{\text{BH}}-M_{\text{def}}$

A final remark concerns the possible correlation between M_{BH} and the mass deficit M_{def} inside the core. This measures how much mass has been expelled from the core during its formation and is computed by taking a Sersic profile which reproduces the SB profile outside the core and integrate the luminosity difference L_{def} between this Sersic function and the best-fit Core-Sersic up to infinity (see S. P. Rusli et al. 2013). The missing light in the centre can then be turned into M_{def} using the dynamical mass-to-light ratio.

S. P. Rusli et al. (2013) computed the mass deficit for a sample of 23 core-galaxies with dynamical M_{BH} estimates (see their Table 4), finding that most galaxies show deficits below $10M_{\text{BH}}$, consistent with a number of mergers $N_{\text{mer}} < 2$. In Fig. 6a we plot the deficits from our sample together with those from S. P. Rusli et al. (2013) and NGC1272 (R. Saglia et al. 2024). The correlation between M_{BH} and M_{def} is not particularly strong: the Spearman’s correlation coefficient is only 0.36. Fig. 6b shows the histogram of the mass deficits scaled to the respective M_{BH} value. Simulations

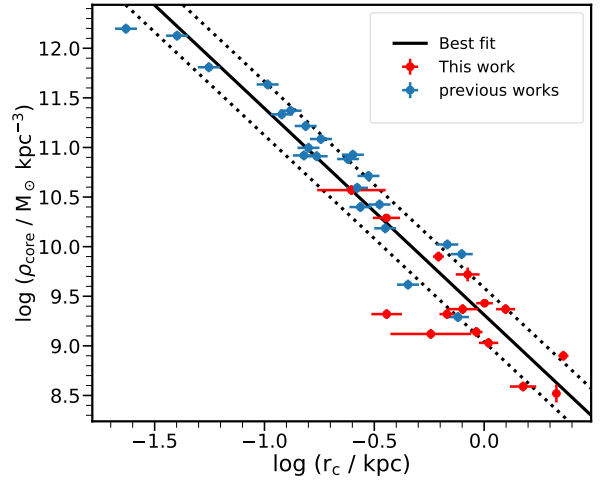


Figure 5. Same as Figs. 2 and 4 but the correlation between core density ρ_{core} and core size r_c is shown.

show (A. Gualandris & D. Merritt 2008) that a single dry merger can generate a deficit of up to $5M_{\text{BH}}$. Therefore, in the most cases the missing mass can be accounted for assuming only two major, dry mergers per galaxy, agreeing with the results of S. P. Rusli et al. (2013).

3.7. Can UMBHs in core-less galaxies exist?

J. W. Nightingale et al. (2023) report a 30-billion solar mass BH in a core-less galaxy. In this work, we found a second example: A2107 does not show any resolved core (de Nicola et al. in prep.), has the *second most massive UMBH of the whole sample* and the largest σ . If the presence of UMBHs does not necessarily require a core elliptical, then the demography and the evolution of high-mass end of the BH mass function cannot be determined from a census of core-less galaxies but requires dedicated surveys of respective core-less galaxies, with important consequences in the context of Pulsar Time Array (PTA) data. In fact, a gravitational-wave background is expected from the distribution of merging SMBH binaries. In particular, the properties of the mergers - mass of the progenitors, spin - shape the spectrum and the amplitude of the background (E. R. Liepold & C.-P. Ma 2024). Such candidates can be identified using the $M_{\text{BH}}-M_*$ relation, which - in contrast with the $M_{\text{BH}}-\sigma$ - works well at the high-mass end (see Sec. 3.3). The remaining question is how these systems can exist. A simple, possible explanation would be the following: while the widely accepted evolution scenario leading to the formation of massive ETGs suggests that these accrete mass through dry mergers in the latest

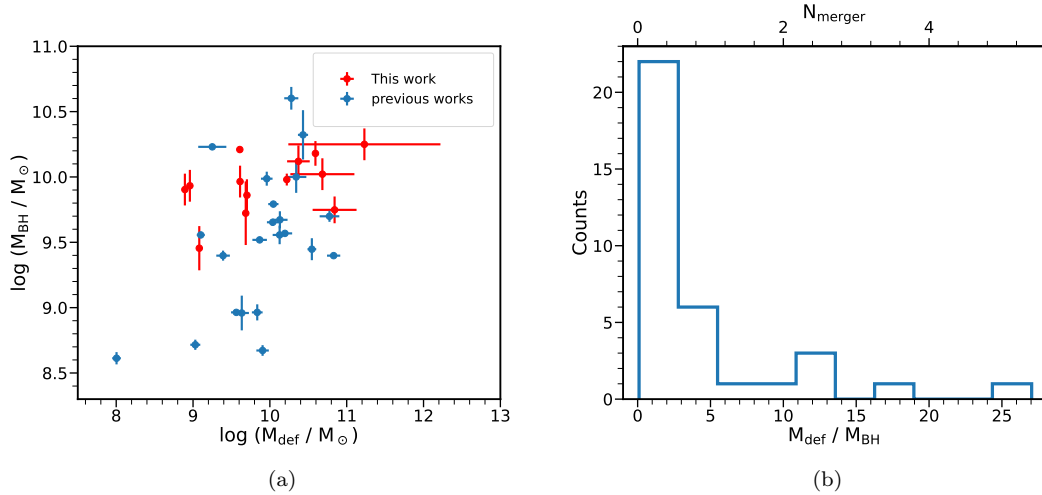


Figure 6. *Left:* Plot of the mass deficit M_{def} inside the core against M_{BH} . No strong correlation is found. *Right:* M_{def} values scaled to the respective M_{BH} estimates. The top axis shows the smallest number of mergers needed to generate M_{def} according to A. Gualandris & D. Merritt (2008).

phases (R. Bender et al. 1992; J. Kormendy & R. Bender 1996), a small number of galaxies may well have experienced late wet mergers as well or growth from cooling-flow gas, resulting in cuspy profiles *and* UMBHs.

4. CONCLUSIONS

We have shown that the canonical $M_{\text{BH}}-\sigma$ relation is inadequate for predicting black hole masses at the high-mass end, and the effect is particularly severe for BCGs, given their low central velocity dispersion. In contrast, the core size predicts M_{BH} much more accurately and allows for the rapid identification of galaxies potentially hosting a massive BH, requiring only photometric data. While systems with large cores and small black holes can exist - with two confirmed detections (A1201 and A2107) - the presented scaling relations and the selection of the targets based only on their core-size, suggest that such systems are rare. On the other side, we do find massive or even ultra-massive black-holes in core-less galaxies, suggesting that even the most massive galaxy can undergo merging processes which can re-form a cuspy SB profile. These galaxies can be identified using the $M_{\text{BH}} - M_*$ relation.

We have also discussed the connection between the $M_{\text{BH}} - r_c$ correlation and the even tighter correlation between r_{SOI} and r_c . This provides a direct link to the black-hole binary model of core formation. This model can plausibly explain the $M_{\text{BH}} - r_c$ correlation and we have shown how the homology properties and in particular the central densities of the progenitor galaxies influence the expected slope of the relation.

We plan to extend the study of cores and of the evolution of black holes and host galaxies to higher redshift,

up to $z = 1$, with data from the Euclid telescope. Our discussion of the role of progenitor properties could help providing clues how to interpret any potential evolution in the various M_{BH} -core correlations.

ACKNOWLEDGEMENTS

Computations were performed on the HPC systems Raven and Cobra at the Max Planck Computing and Data Facility.

The LBT is an international collaboration among institutions in the United States, Italy and Germany. LBT Corporation partners are: LBT Beteiligungsgesellschaft, Germany, representing the Max-Planck Society, the Astrophysical Institute Potsdam, and Heidelberg University; The University of Arizona on behalf of the Arizona university system; Istituto Nazionale di Astrofisica, Italy; The Ohio State University, and The Research Corporation, on behalf of The University of Notre Dame, University of Minnesota and University of Virginia.

modsCCDRed was developed for the MODS1 and MODS2 instruments at the Large Binocular Telescope Observatory, which were built with major support provided by grants from the U.S. National Science Foundation's Division of Astronomical Sciences Advanced Technologies and Instrumentation (AST-9987045), the NSF/NOAO TSIP Program, and matching funds provided by the Ohio State University Office of Research and the Ohio Board of Regents. Additional support for modsCCDRed was provided by NSF Grant AST-1108693. This paper made use of the modsIDL spectral data reduction pipeline developed in part with funds provided by NSF Grant AST-1108693 and a generous gift from OSU Astronomy alumnus David G.

Galaxy	M_{BH} ($10^9 M_{\odot}$)	r_c (kpc)	r_{SOI} (kpc)	σ (km s $^{-1}$)	ρ_{core} ($10^9 M_{\odot} \text{ kpc}^{-3}$)	$M_{\text{gal,2D}}$ ($10^{11} M_{\odot}$)	$M_{\text{gal,Sersic}}$ ($10^{11} M_{\odot}$)	M_{def} ($10^9 M_{\odot}$)
A160	13.2 ± 3.7	0.921 ± 0.060	1.50 ± 0.13	302.3 ± 7.3	1.380 ± 0.069	25.4 ± 2.3	13.5 ± 1.2	23.5 ± 3.5
A240	9.2 ± 2.6	0.678 ± 0.053	1.26 ± 0.13	258.2 ± 4.3	2.09 ± 0.10	10.9 ± 1.1	10.0 ± 1.0	4.09 ± 0.61
A292	13.8 ± 3.9	$1.25 \pm 0.12^{**}$	1.06 ± 0.13	311.0 ± 7.3	2.34 ± 0.12	33.3 ± 2.3	55.3 ± 3.9	-
A399	7.2 ± 2.0	1.50 ± 0.21	1.64 ± 0.13	289 ± 10	0.389 ± 0.019	100 ± 11	118 ± 13	5.03 ± 0.74
A592	8.6 ± 2.4	0.57 ± 0.24	1.26 ± 0.13	278.3 ± 5.1	1.318 ± 0.066	55.8 ± 3.7	92.8 ± 6.1	0.91 ± 0.14
A634	5.6 ± 1.3	0.249 ± 0.088	0.367 ± 0.063	266.9 ± 4.1	37.2 ± 1.9	8.07 ± 0.90	13.4 ± 1.5	69.6 ± 7.1
A1185	11.2 ± 3.1	$1.05 \pm 0.10^{**}$	1.50 ± 0.13	301.9 ± 6.4	1.072 ± 0.054	12.8 ± 1.1	14.4 ± 1.2	-
A1314	5.3 ± 3.0	0.619 ± 0.035	0.54 ± 0.15	277.3 ± 5.6	7.94 ± 0.40	9.75 ± 0.34	6.35 ± 0.22	4.85 ± 0.39
A1749	10.5 ± 2.9	0.84 ± 0.10	0.8404 ± 0.0040	286.7 ± 3.7	5.25 ± 0.37	14.25 ± 0.87	15.86 ± 0.97	48 ± 10
A1775	15.1 ± 3.3	2.133 ± 0.088	2.14 ± 0.20	336 ± 11	0.331 ± 0.030	76.0 ± 4.0	30.3 ± 1.6	39.17 ± 0.38
A2107	22.4 ± 3.3	-	1.04 ± 0.19	373.1 ± 8.1	14.45 ± 0.87	55.9 ± 2.5	43.97 ± 2.0	-
A2147	16.21 ± 0.90	0.80 ± 0.13	1.38 ± 0.12	266.3 ± 6.1	2.34 ± 0.12	13.9 ± 2.3	2.66 ± 0.44	4.06 ± 0.70
A2256	24.7 ± 6.9	2.29 ± 0.12	1.86 ± 0.13	320.3 ± 8.1	0.890 ± 0.027	62.5 ± 2.2	42.78 ± 1.5	170 ± 26
A2319	8.0 ± 2.3	0.360 ± 0.058	0.994 ± 0.13	386.0 ± 9.3	2.09 ± 0.10	95.2 ± 2.6	32.81 ± 0.91	0.78 ± 0.12
A2388	9.6 ± 1.0	1.00 ± 0.087	0.876 ± 0.050	234.1 ± 5.1	2.69 ± 0.11	48.5 ± 2.4	41.0 ± 2.0	16.61 ± 0.25
A2506	2.8 ± 1.1	0.359 ± 0.051	0.324 ± 0.042	235.1 ± 5.6	19.50 ± 0.39	9.01 ± 0.54	14.11 ± 0.85	1.21 ± 0.11

Table 1. The 16 BCGs considered throughout this work. *Col. 1:* BCG name; *Col. 2:* Black Hole mass; *Col. 3:* Core size. The double ** denotes estimates obtained using the cusp radius instead of the break radius; *Col. 4:* BH Sphere of influence from integrated mass profiles; *Col. 5:* Velocity dispersion; *Col. 6:* Core density; *Cols. 7-8:* Galaxy masses from 2D profiles and Sersic 1D fits, respectively; *Col. 9:* The mass deficit inside the core.

Price through the Price Fellowship in Astronomical Instrumentation.

This work makes use of the data products from the HST image archive.

REFERENCES

- Bender, R., Burstein, D., & Faber, S. M. 1992, ApJ, 399, 462, doi: [10.1086/171940](https://doi.org/10.1086/171940)
- Boylan-Kolchin, M., Ma, C.-P., & Quataert, E. 2006, MNRAS, 369, 1081, doi: [10.1111/j.1365-2966.2006.10379.x](https://doi.org/10.1111/j.1365-2966.2006.10379.x)
- Cappellari, M. 2016, ARA&A, 54, 597, doi: [10.1146/annurev-astro-082214-122432](https://doi.org/10.1146/annurev-astro-082214-122432)
- Carollo, C. M., Franx, M., Illingworth, G. D., & Forbes, D. A. 1997, ApJ, 481, 710, doi: [10.1086/304060](https://doi.org/10.1086/304060)
- de Nicola, S., Marconi, A., & Longo, G. 2019, MNRAS, 490, 600, doi: [10.1093/mnras/stz2472](https://doi.org/10.1093/mnras/stz2472)
- de Nicola, S., Saglia, R. P., Thomas, J., Dehnen, W., & Bender, R. 2020, MNRAS, 496, 3076, doi: [10.1093/mnras/staa1703](https://doi.org/10.1093/mnras/staa1703)
- de Nicola, S., Thomas, J., Saglia, R. P., et al. 2024, MNRAS, 530, 1035, doi: [10.1093/mnras/stae806](https://doi.org/10.1093/mnras/stae806)
- Dullo, B. T., & Graham, A. W. 2014, MNRAS, 444, 2700, doi: [10.1093/mnras/stu1590](https://doi.org/10.1093/mnras/stu1590)
- Ebisuzaki, T., Makino, J., & Okumura, S. K. 1991, Nature, 354, 212, doi: [10.1038/354212a0](https://doi.org/10.1038/354212a0)
- Faber, S. M., Tremaine, S., Ajhar, E. A., et al. 1997, AJ, 114, 1771, doi: [10.1086/118606](https://doi.org/10.1086/118606)
- Ferrarese, L., & Merritt, D. 2000, ApJL, 539, L9, doi: [10.1086/312838](https://doi.org/10.1086/312838)
- Frigo, M., Naab, T., Rantala, A., et al. 2021, MNRAS, 508, 4610, doi: [10.1093/mnras/stab2754](https://doi.org/10.1093/mnras/stab2754)
- Gebhardt, K., Bender, R., Bower, G., et al. 2000, ApJL, 539, L13, doi: [10.1086/312840](https://doi.org/10.1086/312840)
- Gualandris, A., & Merritt, D. 2008, ApJ, 678, 780, doi: [10.1086/586877](https://doi.org/10.1086/586877)
- Hopp, U., Bender, R., Grupp, F., et al. 2010, in Society of Photo-Optical Instrumentation Engineers (SPIE) Conference Series, Vol. 7733, Ground-based and Airborne Telescopes III, ed. L. M. Stepp, R. Gilmozzi, & H. J. Hall, 773307, doi: [10.1117/12.856461](https://doi.org/10.1117/12.856461)
- King, A., & Pounds, K. 2015, ARA&A, 53, 115, doi: [10.1146/annurev-astro-082214-122316](https://doi.org/10.1146/annurev-astro-082214-122316)
- Kluge, M., & Bender, R. 2023, ApJS, 267, 41, doi: [10.3847/1538-4365/ace052](https://doi.org/10.3847/1538-4365/ace052)
- Kluge, M., Bender, R., Riffeser, A., et al. 2021, ApJS, 252, 27, doi: [10.3847/1538-4365/abcda6](https://doi.org/10.3847/1538-4365/abcda6)
- Kluge, M., Neureiter, B., Riffeser, A., et al. 2020, ApJS, 247, 43, doi: [10.3847/1538-4365/ab733b](https://doi.org/10.3847/1538-4365/ab733b)
- Kormendy, J., & Bender, R. 1996, ApJL, 464, L119, doi: [10.1086/310095](https://doi.org/10.1086/310095)
- Kormendy, J., & Bender, R. 2009, ApJL, 691, L142, doi: [10.1088/0004-637X/691/2/L142](https://doi.org/10.1088/0004-637X/691/2/L142)
- Kormendy, J., & Bender, R. 2013, ApJL, 769, L5, doi: [10.1088/2041-8205/769/1/L5](https://doi.org/10.1088/2041-8205/769/1/L5)
- Kormendy, J., & Ho, L. C. 2013, ARA&A, 51, 511, doi: [10.1146/annurev-astro-082708-101811](https://doi.org/10.1146/annurev-astro-082708-101811)
- Lang-Bardl, F., Bender, R., Goessl, C., et al. 2016, in Society of Photo-Optical Instrumentation Engineers (SPIE) Conference Series, Vol. 9908, Ground-based and Airborne Instrumentation for Astronomy VI, ed. C. J. Evans, L. Simard, & H. Takami, 990844, doi: [10.1117/12.2232039](https://doi.org/10.1117/12.2232039)

- Lauer, T. R., Gebhardt, K., Faber, S. M., et al. 2007, *ApJ*, 664, 226, doi: [10.1086/519229](https://doi.org/10.1086/519229)
- Liepold, E. R., & Ma, C.-P. 2024, *ApJL*, 971, L29, doi: [10.3847/2041-8213/ad66b8](https://doi.org/10.3847/2041-8213/ad66b8)
- Lipka, M., & Thomas, J. 2021, *MNRAS*, 504, 4599, doi: [10.1093/mnras/stab1092](https://doi.org/10.1093/mnras/stab1092)
- Magorrian, J., Tremaine, S., Richstone, D., et al. 1998, *AJ*, 115, 2285, doi: [10.1086/300353](https://doi.org/10.1086/300353)
- Marconi, A., & Hunt, L. K. 2003, *ApJL*, 589, L21, doi: [10.1086/375804](https://doi.org/10.1086/375804)
- McConnell, N. J., Ma, C.-P., Murphy, J. D., et al. 2012, *ApJ*, 756, 179, doi: [10.1088/0004-637X/756/2/179](https://doi.org/10.1088/0004-637X/756/2/179)
- Mehrgan, K., Thomas, J., Saglia, R., et al. 2019, *ApJ*, 887, 195, doi: [10.3847/1538-4357/ab5856](https://doi.org/10.3847/1538-4357/ab5856)
- Mehrgan, K., Thomas, J., Saglia, R., Parikh, T., & Bender, R. 2023, *ApJ*, 948, 79, doi: [10.3847/1538-4357/acbf2e](https://doi.org/10.3847/1538-4357/acbf2e)
- Melo-Carneiro, C. R., Collett, T. E., Oldham, L. J., et al. 2025, *MNRAS*, 541, 2853, doi: [10.1093/mnras/staf1036](https://doi.org/10.1093/mnras/staf1036)
- Merritt, D. 2006, *ApJ*, 648, 976, doi: [10.1086/506139](https://doi.org/10.1086/506139)
- Naab, T., Johansson, P. H., & Ostriker, J. P. 2009, *ApJL*, 699, L178, doi: [10.1088/0004-637X/699/2/L178](https://doi.org/10.1088/0004-637X/699/2/L178)
- Neureiter, B., Thomas, J., Rantala, A., et al. 2023, *ApJ*, 950, 15, doi: [10.3847/1538-4357/accffa](https://doi.org/10.3847/1538-4357/accffa)
- Neureiter, B., Thomas, J., Saglia, R., et al. 2021, *MNRAS*, 500, 1437, doi: [10.1093/mnras/staa3014](https://doi.org/10.1093/mnras/staa3014)
- Nightingale, J. W., Smith, R. J., He, Q., et al. 2023, *MNRAS*, 521, 3298, doi: [10.1093/mnras/stad587](https://doi.org/10.1093/mnras/stad587)
- Rantala, A., Johansson, P. H., Naab, T., Thomas, J., & Frigo, M. 2018, *ApJ*, 864, 113, doi: [10.3847/1538-4357/aada47](https://doi.org/10.3847/1538-4357/aada47)
- Rantala, A., Johansson, P. H., Naab, T., Thomas, J., & Frigo, M. 2019, *ApJL*, 872, L17, doi: [10.3847/2041-8213/ab04b1](https://doi.org/10.3847/2041-8213/ab04b1)
- Rawlings, A., Keitaanranta, A., Matteredo, M., et al. 2025, *MNRAS*, 537, 3421, doi: [10.1093/mnras/staf238](https://doi.org/10.1093/mnras/staf238)
- Rusli, S. P., Erwin, P., Saglia, R. P., et al. 2013, *AJ*, 146, 160, doi: [10.1088/0004-6256/146/6/160](https://doi.org/10.1088/0004-6256/146/6/160)
- Saglia, R., Mehrgan, K., de Nicola, S., et al. 2024, *A&A*, 692, A124, doi: [10.1051/0004-6361/202452548](https://doi.org/10.1051/0004-6361/202452548)
- Saglia, R. P., Opitsch, M., Erwin, P., et al. 2016, *ApJ*, 818, 47, doi: [10.3847/0004-637X/818/1/47](https://doi.org/10.3847/0004-637X/818/1/47)
- Sérsic, J. L. 1963, *Boletín de la Asociación Argentina de Astronomía La Plata Argentina*, 6, 41
- Shankar, F., Bernardi, M., Sheth, R. K., et al. 2016, *MNRAS*, 460, 3119, doi: [10.1093/mnras/stw678](https://doi.org/10.1093/mnras/stw678)
- Shankar, F., Bernardi, M., Roberts, D., et al. 2025, *MNRAS*, 541, 2070, doi: [10.1093/mnras/staf747](https://doi.org/10.1093/mnras/staf747)
- Thomas, J., & Lipka, M. 2022, *MNRAS*, doi: [10.1093/mnras/stac1581](https://doi.org/10.1093/mnras/stac1581)
- Thomas, J., Ma, C.-P., McConnell, N. J., et al. 2016, *Nature*, 532, 340, doi: [10.1038/nature17197](https://doi.org/10.1038/nature17197)
- Thomas, J., Saglia, R. P., Bender, R., Erwin, P., & Fabricius, M. 2014, *ApJ*, 782, 39, doi: [10.1088/0004-637X/782/1/39](https://doi.org/10.1088/0004-637X/782/1/39)
- Tremaine, S., Gebhardt, K., Bender, R., et al. 2002, *ApJ*, 574, 740, doi: [10.1086/341002](https://doi.org/10.1086/341002)
- Trujillo, I., Erwin, P., Asensio Ramos, A., & Graham, A. W. 2004, *AJ*, 127, 1917, doi: [10.1086/382712](https://doi.org/10.1086/382712)
- van den Bosch, R. C. E. 2016, *ApJ*, 831, 134, doi: [10.3847/0004-637X/831/2/134](https://doi.org/10.3847/0004-637X/831/2/134)